Urinary complement proteins in IgA nephropathy progression from a relative quantitative proteomic analysis

Xia Niu [Equal first author, 1] , **Shuyu Zhang** [Equal first author, 2] , **Chen Shao** [1] , **Zhengguang Guo** [1] , **Jianqiang Wu** [1] , **Jianling Tao** [2] , **Ke Zheng** [2] , **Wenling Ye** [2] , **Guangyan Cai** [3] , **Wei Sun** [Corresp., 1] , **Mingxi Li** [Corresp. 2]

[1] Core Facility of Instruments, Institute of Basic Medical Sciences, Chinese Academy of Medical Sciences, School of Basic Medicine, Peking Union Medical College, Beijing, China

[2] Department of Nephrology, State Key Laboratory of Complex Severe and Rare Diseases, Peking Union Medical College Hospital, Chinese Academy of Medical Science and Peking Union Medical College, Beijing, China

[3] Department of Nephrology, The First Medical Centre, Chinese PLA General Hospital, Medical School of Chinese PLA, Beijing, China

Corresponding Authors: Wei Sun, Mingxi Li
Email address: sunwei@ibms.pumc.edu.cn, mingxili@hotmail.com

Aim: IgA nephropathy (IgAN) is one of the leading causes of end-stage renal disease (ESRD). Urine is a source of noninvasive biomarkers of body fluids that are used for measuring renal injury. This study aimed to analyse the complements during IgAN progression by quantitative proteomic strategy.**Methods:** In the discovery phase, we analysed 22 IgAN patients who were divided into three groups (IgAN 1-3) according to the estimated glomerular filtration rate. The other 8 patients with primary membranous nephropathy (pMN) were set as controls. Isobaric tags for relative and absolute quantitation (iTRAQ) labelling coupled with liquid chromatography-tandem mass spectrometry was applied to analyse global urinary protein expression. In the validation phase, Western blotting and parallel reaction monitoring (PRM) were used to verify the iTRAQ results in an independent cohort (N=64).**Results:** In the discovery phase, 747 proteins were identified in the urine of IgAN and pMN patients. There are different urine protein profiles in IgAN and pMN, and the bioinformatics analysis revealed that the complement and coagulation pathways were most activated. We totally identified 27 urinary complements related to IgAN. The relative abundance of C3, the membrane attack complex (MAC) and the complement regulatory proteins of the alternative pathway (AP), MBL and MASP1 of the lectin pathway (LP) were increased during IgAN progression, especially MAC, which was found to be involved prominently in disease progression. Alpha-N-acetylglucosaminidase (NAGLU) and α-galactosidase A (GLA) were validated by Western blot and consistent with iTRAQ. By PRM analysis, 10 proteins with significant differences were validated, and these results were consistent with the iTRAQ results. Complement (CFB) and complement component C8 alpha chain (C8A) presented increasing abundance with the progression of IgAN. The combination of CFB and MAdCAM-1 showed excellent

area under the curve values to discriminate the progression of IgAN.**Conclusion**: There were abundant complement components in the urine of IgAN patients, indicating that the activation of AP and LP is involved in IgAN progression. Urinary complements may be used as biomarkers for evaluating IgAN progression in the future.

2

Urinary complement proteins in IgA nephropathy progression from a relative

quantitative proteomic analysis

Xia Niu1#, Shuyu Zhang2#, Chen Shao1, Zhengguang Guo1, Jianqiang Wu1, Jianling Tao2, Ke Zheng2, Wenling Ye2, Guangyan Cai3, Wei Sun1*, Mingxi Li2*

1. Core Facility of Instruments, Institute of Basic Medical Sciences, Chinese Academy of Medical Sciences, School of Basic Medicine, Peking Union Medical College, Beijing, China.

2. Department of Nephrology, State Key Laboratory of Complex Severe and Rare Diseases, Peking Union Medical College Hospital, Chinese Academy of Medical Science and Peking Union Medical College, Beijing, China.

3. Department of Nephrology, The First Medical Centre, Chinese PLA General Hospital, Medical School of Chinese PLA, Beijing, China.

Corresponding author

Wei Sun1*

Core Facility of Instruments, Institute of Basic Medical Sciences, Chinese Academy of Medical Sciences, School of Basic Medicine, Peking Union Medical College, Beijing, China.

E-mail: sunwei@ibms.pumc.edu.cn

Mingxi Li2*

Department of Nephrology, State Key Laboratory of Complex Severe and Rare Diseases, Peking Union Medical College Hospital, Chinese Academy of Medical Science and Peking Union Medical College, Beijing, China.

24 Tel: 8610-65295058

25 E-mail: mingxili@hotmail.com

26 **The first author**

27 **Xia Niu1#**

28 Core Facility of Instruments, Institute of Basic Medical Sciences, Chinese Academy of Medical

29 Sciences, School of Basic Medicine, Peking Union Medical College, Beijing, China

30 E-mail: bante727@163.com

31 **Shuyu Zhang2#**

32 Department of Nephrology, State Key Laboratory of Complex Severe and Rare Diseases, Peking

33 Union Medical College Hospital, Chinese Academy of Medical Science and Peking Union

34 Medical College, Beijing, China.

35 E-mail: zhang__shuyu@163.com

39 **Footnote:** The current work institution of Chen Shao is State Key Laboratory of Proteomics,

40 Beijing Proteome Research Center, National Center for Protein Sciences, Beijing Institute of

41 Lifeomics, Beijing, China. The current work institution of Jianqiang Wu is Medical Research

42 Center, State Key Laboratory of Complex Severe and Rare Diseases, Peking Union Medical

43 College Hospital, Chinese Academy of Medical Science and Peking Union Medical College,

44 Beijing, China. The present work institution of Jianling Tao is Division of Nephrology, Stanford

45 University, Palo alto, CA, USA.

51   **Running title: Urine complements of IgAN patients**

52   **Abstract**

53   **Aim:** IgA nephropathy (IgAN) is one of the leading causes of end-stage renal disease (ESRD).

54   Urine is a source of noninvasive biomarkers of body fluids that are used for measuring renal injury.

55   This study aimed to analyse the complements during IgAN progression by quantitative proteomic

56   strategy.

57   **Methods:** In the discovery phase, we analysed 22 IgAN patients who were divided into three

58   groups (IgAN 1-3) according to the estimated glomerular filtration rate. The other 8 patients with

59   primary membranous nephropathy (pMN) were set as controls. Isobaric tags for relative and

60   absolute quantitation (iTRAQ) labelling coupled with liquid chromatography-tandem mass

61   spectrometry was applied to analyse global urinary protein expression. In the validation phase,

62   Western blotting and parallel reaction monitoring (PRM) were used to verify the iTRAQ results

63   in an independent cohort (N=64).

64   **Results:** In the discovery phase, 747 proteins were identified in the urine of IgAN and pMN

65   patients. There are different urine protein profiles in IgAN and pMN, and the bioinformatics

66   analysis revealed that the complement and coagulation pathways were most activated. We totally

67   identified 27 urinary complements related to IgAN. The relative abundance of C3, the membrane

68   attack complex (MAC) and the complement regulatory proteins of the alternative pathway (AP),

69   MBL and MASP1 of the lectin pathway (LP) were increased during IgAN progression, especially

70   MAC, which was found to be involved prominently in disease progression. Alpha-N-

71   acetylglucosaminidase (NAGLU) and α-galactosidase A (GLA) were validated by Western blot

72   and consistent with iTRAQ. By PRM analysis, 10 proteins with significant differences were

73   validated, and these results were consistent with the iTRAQ results. Complement (CFB) and

74   complement component C8 alpha chain (C8A) presented increasing abundance with the

75   progression of IgAN. The combination of CFB and MAdCAM-1 showed excellent area under the

76   curve values to discriminate the progression of IgAN.

77   **Conclusion**: There were abundant complement components in the urine of IgAN patients,

78   indicating that the activation of AP and LP is involved in IgAN progression. Urinary complements

79   may be used as biomarkers for evaluating IgAN progression in the future.

80   **Keywords:** Complement proteins; IgA nephropathy; α-N-acetylglucosaminidase; Proteomics;

81   Urine;

82

83

84

85

86   **1. Introduction**

87   IgA nephropathy (IgAN) is the most common primary glomerulonephropathy worldwide, and

88   20-30% of patients with IgAN progress to end-stage renal disease within 10 years of disease onset

89   [1]. The four-hit hypothesis of IgAN pathogenesis [2] involves elevated serum galactose-deficient

90   IgA1 (Gd-IgA1), IgG or IgA antibody specific to Gd-IgA1, formation of immune complexes (ICs)

91   and IC deposits predominantly on the glomerular mesangium, leading to inflammation,

92 complement activation, mesangial hypercellularity and glomerulosclerosis.

93 Activation of the complement cascade is involved in the pathogenesis of IgAN. The

94 alternative and lectin pathways dominate the complement activation of IgAN [3]. However,

95 previous studies have not revealed the role of complement proteins in IgAN progression. Data

96 from mass spectrometry (MS) analysis in kidney biopsy samples have demonstrated that the

97 complement pathways are involved in IgAN [4].

98 As a noninvasively accessible, low background and relatively stable biofluid, urine is an ideal

99 source for biomarker discovery via proteomic approaches. Urinary proteomics could be used to

100 analyse protein profiles and assess pathogenetic mechanisms in an overall view involved in disease

101 progression. Previously, some urinary proteomic studies in IgAN have been devoted to candidate

102 biomarker discovery [5,6], but there is no study on urinary proteomic profile changes during IgAN

103 progression.

104 The proteomic study usually includes two phases, discovery and validation. In the discovery

105 phase, the samples were analysed by an untargeted proteomics approach to identify the

106 differentially expressed proteins, which may be related to disease mechanisms, drug targets or

107 disease biomarkers [7]. In the validation phase, the differential proteins were analysed by targeted

108 methods, including Western blotting, ELISA, and PRM, in another cohort to validate the results

109 of the discovery phase [8].

110 The use of isobaric tags for relative and absolute quantification (iTRAQ) is a new technique

111 in quantitative proteomics to identify and quantify protein expression levels. Parallel reaction

112 monitoring (PRM) can distinguish between interference information and real signals and has

113 greater selectivity to detect target proteins, often used for verification of iTRAQ differential

114 proteins.

115   In this study, urine samples were collected from IgAN patients with different disease severities

116   and primary membranous nephropathy (pMN) patients. After removing fourteen highly abundant

117   proteins, urine samples of IgAN and pMN patients were analysed by iTRAQ labelling coupled

118   with liquid chromatography-tandem mass spectrometry (2D-LC/MS/MS) for quantitative

119   proteome analysis. Furthermore, PRM was also used to validate the differentially expressed

120   proteins. The aim of this study was to analyse the entire urinary protein profiles in IgAN patients

121   with different disease stages to assess whether the overall urinary complement expression profile

122   changes with disease progression.

123   **2. Materials and Methods**

124   **2.1 Reagents and instruments**

125   HPLC-grade acetonitrile (ACN), trifluoroacetic acid, formic acid, ammonium bicarbonate,

126   iodoacetamide (IAA), and dithiothreitol (DTT) were all purchased from Sigma (St. Louis, MO,

127   USA). Sequencing-grade trypsin was purchased from Promega (Madison, WI, USA). The 4-plex

128   iTRAQ reagents were purchased from ABsciex (Framingham, MA, USA). An Orbitrap Fusion

129   Lumos Tribrid mass spectrometer coupled with an EASY-nLC 1000 HPLC system was purchased

130   from Thermo (Thermo Fisher Scientific, MA, USA) and then applied for proteome analysis in

131   both discovery and validation phases. For Western blotting, primary antibodies against α-N-

132   acetylglucosaminidase (NAGLU, ab72178) and α-galactosidase A (GLA, ab168341) were

133   purchased from Abcam (Cambridge, UK).

134   **2.2 Patients and urine samples**

135   All the patients enrolled in this study were diagnosed with IgAN by kidney biopsy. Fresh urine

136   samples were collected on the morning of kidney biopsy. For the discovery cohort, the sample

137   collection duration was from August 2014 to January 2017, and the sample collection of the

138 validation cohort was from November 2019 to July 2021. The urine was centrifuged at 3000 × g

139 for 30 min. The sediment was discarded, and the supernatant was stored at -80 °C. This study was

140 approved by the Ethics Committee of Peking Union Medical College Hospital (approval number:

141 JS-2573), and the enrolled patients signed informed consent forms. The amount of 24-h urine

142 proteins (24hUP), serum creatinine (SCr), and estimated glomerular filtration rate (eGFR) of

143 patients were evaluated. The CKD-EPI equation was used to estimate the eGFR as described

144 previously [9]. The clinical characteristics of the patients in the discovery and validation phases

145 are shown in Table 1. The pMN was diagnosed by renal pathology (light microscopy,

146 immunofluorescence and electron microscopy). Secondary MN due to infection, malignant

147 neoplasms, rheumatologic disease, drugs, and other systemic causes was ruled out. In both the

148 discovery and validation phases, IgAN patients were divided into three subgroups based on the

149 eGFR, namely, IgAN-1 (eGFR: > 90 ml/min/1.73 m^2), IgAN-2 (eGFR: 60-90 ml/min/1.73 m^2)

150 and IgAN-3 (eGFR: 30-60 ml/min/1.73 m^2). Two nephropathologists evaluated renal biopsy

151 samples independently according to the Oxford Classification of IgA nephropathy from the IgA

152 Nephropathy Classification Working Group in 2016 [10].

153 **2.3 Urinary protein extraction**

154 The urine supernatants were precipitated by ethanol overnight at −20 °C. After centrifugation at

155 12,000 × g for 30 min, the pellets were resuspended in lysis buffer (7 M urea, 2 M thiourea, 0.1 M

156 DTT, 50 mM Tris). The protein concentration of each sample was measured using the Bradford

157 method. In the discovery phase, highly abundant proteins were removed from urine protein

158 samples using an Agilent Mars14 chromatography column following the manufacturers' protocol

159 (Agilent, Palo Alto, CA, USA). Equal amounts of total urine protein from each individual patient

160 within one patient group were pooled together. Finally, four pooled protein samples were formed

161   from IgAN 1-3 and pMN patients for proteomic analysis.

162   **2.4 Protein digestion and iTRAQ labelling**

163   Each sample was digested using the filter-aided sample preparation method (FASP) [11].

164   Protein samples were denatured with 20 mM DTT at 37 °C for 1 h and alkylated with 50 mM IAA

165   in the dark for 45 min. Then, the samples were loaded onto filter devices with a cut-off of 10 kD

166   (Pall, Port Washington, NY, USA) and centrifuged at 14,000 g at 18 °C. After washing twice with

167   UA (8 M urea in 0.1 M Tris-HCl, pH 8.5) and twice with 25 mM NH_4HCO_3, the samples were

168   redissolved in 25 mM NH4HCO3 and digested with trypsin (enzyme to protein ratio of 1:50) at

169   37 °C overnight. The digested peptides were collected as a filtrate and desalted using Oasis HLB

170   C18 cartridges (Waters, Milford, MA). The IgAN 1-3 and MN samples were individually labelled

171   with 114, 115, 116 and 117 4-plex iTRAQ chemistry according to the manufacturer's protocol

172   (ABsciex, USA).

173   **2.5 2D-LC/MS/MS**

174   2D-LC–MS/MS detection was performed as described previously [12]. The pooled mixture of

175   iTRAQ-labelled samples was fractionated using a high-pH RPLC column from Waters (4.6 mm ×

176   250 mm, Xbridge C18, 3 μm). The samples were loaded onto the column in buffer A1 (H_2O, pH

177   = 10) and then eluted under a gradient of 5–25% buffer B1 (90% ACN, pH =10) for 60 min with

178   flow rate at 1 mL/min. The eluted peptides were collected at fractions by minute and dried by

179   vacuum evaporation for further redissolution. As Guo et.al proposed previously, the 60 dried

180   fractions were resuspended in 0.1% formic acid and then pooled into 20 samples with certain

181   regularity, for example, combining fractions 1, 21, 41 and 2, 22, 42 and so on. Eventually, 20

182   fractions from urinary peptide mixtures were analysed by LC–MS/MS.

183   Each fraction was analysed with a reversed-phase C18 capillary column (75 μm×100 mm).

184 An Orbitrap Fusion Lumos Tribrid mass spectrometer was used to analyse the mixed peptides

185 fractions by two times. A high-sensitivity mode was applied for the acquirement of MS data.

186 Detailed parameters of PRM mode were as followed: data-dependent MS/MS scans per full scan

187 with top-speed mode (3 s), full scans (resolution = 60,000) and MS/MS scans (resolution = 15000),

188 38% HCD collision energy, charge-state screening (charge state of precursors: from +2 to +6),

189 dynamic exclusion (exclusion duration1: 30 s), and maximum injection time (60 ms).

190 **2.8 Western blot analysis**

191 Two candidate proteins associated with glycosylation, NAGLU and GLA, were selected for WB

192 validation in individual urine samples from IgAN and MN patients. Thirty micrograms of urinary

193 protein from each sample was loaded onto 10% SDS–PAGE gels and transferred to PVDF

194 membranes. After blocking in 5% milk for 1 h, the membranes were incubated with primary

195 antibodies at 4 °C overnight. Then, the membranes were washed with TBST four times and

196 incubated with secondary antibodies (diluted 1:5,000 in 5% milk solution) for 1 h at room

197 temperature. The blots of NAGLU and GLA were visualized using enhanced chemiluminescence

198 reagents (Thermo Scientific, USA). The intensity of blots were scanned with an ImageQuant

199 400TM Imager (GE Healthcare Life Sciences, Piscataway, NJ, USA) and protein signals were

200 quantified using the AlphaEaseFC system.

201 **2.6 Parallel reaction monitoring (PRM) analysis**

202 For PRM validation, the different proteins from LC–MS/MS analysis were evaluated in

203 validation cohort consist of 64 IgAN patients. Each sample was analysed in schedule mode. The

204 mixed sample were analysed as quality control (QC) to ensure the availability of data and the

205 stability of the instrument signal for the PRM validation.

206 An Orbitrap Fusion Lumos Tribrid mass spectrometer (Thermo Fisher Scientific, MA, USA)

207   was used for PRM analysis. An RP C18 self-packing capillary LC column (75 mm × 100 mm) was

208   applied to separate the peptides. The elution gradient was 5-30% buffer B1 (0.1% formic acid,

209   99.9% ACN; flow rate, 0.5 ml/min), and peptides were eluted for 45 minutes. The MS data were

210   achieved under the PRM mode with parameters as followed: full scans acquired (resolution:

211   60,000), MS/MS scans (resolution: 15,000), 32% collision energy, dynamic exclusion (30 s),

212   MS/MS scan range (100-1800 m/z), scan time (100 ms), isolation window at 4 Da and schedule

213   window (7 minutes).

214   **2.7 Data processing**

215   Proteome Discover (Thermo Fisher, Waltham, USA; version 2.1) was used for database

216   searching. Proteome data were searched by comparing with the SwissProt human database (20,227

217   entries) assuming trypsin digestion (http://www.ebi.ac.uk/swissprot/). The parent and fragment ion

218   mass tolerances were 10 ppm and 0.05 Da. Carbamidomethyl cysteine was specified as a fixed

219   modification, with two miscleavage sites accepted. Proteins were available with false discovery

220   rate (FDR) lower than 1.0% and also at least two unique peptides identified. The acquired

221   intensities were generally normalized across all runs. The normalization of reference channels

222   were also used to determine a 1:1-fold change. All normalization processing was achieved with

223   medians in multiplicative manner.

224   For the PRM mode, Skyline 21.1 software was used for the selection of the suitable m/z

225   precursor ion to m/z fragment ion transition thereby determining candidate peptides of potential

226   biomarkers. Required data was imported into Skyline software, where the proper data were chosen

227   manually, and the results of peptides from all samples were finally exported. For each sample,

228   total ionic chromatography (TIC) of ions with +2 - +5 charge was settled by Progenesis software.

229   The normalization of each peptide by TIC strength was performed to adjust the errors caused by

230   the quality of sample loading and the intensity of MS signal. The quantitation of the peptides was

231   subsequently analysed.

2.8 Statistical analysis

233   Continuous data are performed with the mean ± standard deviation or median. Categorical data

234   are performed with absolute frequencies and percentages. The Kolmogorov–Smirnov test was

235   performed to evaluate the normality of the distribution. For the quantitative data, one-way analysis

236   of variance (ANOVA) was used to compare the differences for normally distributed data, and non-

237   parametric test was performed for non-normally distributed data. For the categorical variables, chi-

238   square test was used for the comparison among groups. P values < 0.05 were considered as

239   statistically significance. Above data were analysed with SPSS version 26.0 software (SPSS Inc.,

240   Chicago, IL, USA).

241   Receiver operating characteristic (ROC) curves of all the significantly different proteins were

242   achieved by Metaboanalyst software (http://www.metaboanalyst.ca). The combination ROC

243   analysis was analysed with linear SVM algorithm, and the area under the ROC curve (AUC) was

244   also calculated by separately comparing IgAN-2 and IgAN-3 with the IgAN-1 during the

245   validation phase to identify candidate diagnostic markers.

2.9 Bioinformatics analysis

247   Mfuzz analysis was performed to detect different clustering models of protein expression among

248   IgAN groups of different CKD stages in the discovery phase. We applied pathway enrichment

249   analysis to determine the different pathways of the proteins with statistics significance according

250   to the KEGG (Kyoto Encyclopedia of Genes and Genomes) database. Protein interaction networks

251   were constructed to demonstrate the potential association among different pathways. The data

252   analysis was performed in the OmicsBean workbench (http://www.omicsbean.cn). An adjusted P

253   value < 0.05 was considered statistically significant.

254   **3. Results**

255   **3.1 Clinical and pathological characteristics of the patients**

256   In this study, a total of 30 patients were included in the discovery phase, and another independent

257   cohort including 26 and 64 patients was enrolled for WB and PRM validation. The clinical data

258   and pathological characteristics of the patients are summarized in **Table 1**. In the iTRAQ, WB and

259   PRM phases, there were significant differences in SCr and eGFR among the IgAN 1-3 and pMN

260   patient groups. There were significant differences in the T-score of the Oxford classification in the

261   IgAN-3 group compared with the IgAN-1/2 groups in the discovery phase and significant

262   differences in the T-scores of the Oxford classification between the IgAN-3 and IgAN-1 groups in

263   the validation phase (*P* < 0.05) **(Table 1).**

264   **3.2 Bioinformatics analysis of urine proteomes in IgAN and MN patients**

265   The workflow of the urine proteomics analysis is shown in **Figure 1**. Urine samples of IgAN-

266   1, IgAN-2, IgAN-3 and pMN were pooled, and an antibody column was used to remove 14 high-

267   abundance proteins from urine samples prior to proteomic analysis. A total of 747 urinary proteins

268   were identified with at least two unique peptides in both technical replicates using 2D-LC–MS/MS

269   and iTRAQ quantification (**Table S1**). Western blotting for NGALU and GLA was applied in

270   IgAN and MN patients. Furthermore, PRM was used for the targeted quantification of unique

271   peptides from differentially expressed proteins (DEPs) in another IgAN 1-3 cohort.

272   After hierarchical clustering analysis of all urinary proteins identified, it was found that in

273   IgAN 1-3 and pMN, there were different urine protein expression patterns (**Figure 2A**). Mfuzz

274   analysis of 747 urinary proteins in three IgAN subgroups is shown in **Figure 2B**. Among the 4

275   clusters, Cluster 1, consisting of 120 urinary proteins, was increased with IgAN progression, and

276 the main enrichment pathways included complement and coagulation pathways and

277 *Staphylococcus aureus* infection (**Figure 3A**). Protein–protein interaction (PPI) analysis showed

278 that three pathways are mainly related to complement C3, C5-9, complement lectin pathway (LP),

279 mannan-binding lectin (MBL) and alternative pathway (AP) complement regulatory proteins

280 (**Figure 3B**).

281   The expression of 194 proteins in Cluster 2 gradually decreased with decreasing eGFR.

282 Further pathway enrichment analysis showed that Cluster 2 was involved in cell adhesion

283 molecules, ECM-receptor interactions, regulation of the actin cytoskeleton and the PI3K-Akt

284 signalling pathway (**Figure 3C**). PPI analysis demonstrated that collagen and fibronectin in these

285 pathways were downregulated (**Figure 3D**).

286   Both IgAN-1 and pMN patients in this study had similar eGFRs. We compared the urinary

287 proteins of the IgAN1 group with those of the pMN group according to a cut-off value of fold

288 change＞1.50 or ＜0.67, used to indicate differentially expressed proteins. There were 150

289 differentially expressed proteins between the IgAN-1 and pMN groups, 107 of which were

290 upregulated. A clustering analysis of 107 proteins revealed that the main enrichment pathways

291 were regulation of actin cytoskeleton, focal adhesion, protein digestion and absorption. PPI

292 analysis showed that structural proteins, such as collagen 4-6, nectin1 and nectin2, were relatively

293 more highly expressed in abundance than pMN. Moreover, as shown in Table S1, 17 urinary

294 proteins showed differential abundances between pMN and IgAN patients (15 proteins were

295 expressed at higher levels in pMN than in IgAN1-3 patients).

296 **3.3 Urinary complement pattern analysis in IgAN and MN patients**

297   Among the 747 proteins identified in urine, 27 were complement proteins. The urinary

298 complements were divided into 5 categories: the classical pathway (C1 s, C1rL, C1qR, C1 inhibitor

299 SERPING1, C2 and C4), the lectin pathways (MBL, MASP1, MASP2 and Ficolin2), the AP

300 complement regulatory proteins (CFB, CFD, CFH, CFHR2, CFHR4, CFI, DAF and properdin),

301 the membrane attack complex (MAC) in the terminal pathways (C5, C6, C7, C8A, C8B, C8G, C9

302 and MCP) and C3. The abundance of urinary C3, MAC and complement regulatory proteins was

303 increased during the progression of IgAN. MAC compositions increased most significantly, while

304 the classical pathway proteins did not increase with the progression of IgAN. It was noted that for

305 proteins in the LP of the complement cascade, as eGFR declined, MASP1 and MBL were

306 upregulated, while MASP2 and Ficolin2 were downregulated. The abundance of five categories

307 of urinary complement proteins in IgAN-1 patients was similar to that in pMN patients (**Figure 4,**

308 **Table 2**).

309 **3.4 Western blot validation of glycosylation-related proteins**

310 Two proteins involved in glycosylation and glycan modifications (alpha-N-

311 acetylglucosaminidase, NAGLU and alpha-galactosidase A, GLA) were further validated by

312 Western blot in another patient group, including IgAN 1-3 and pMN (**Figure 5, Figure S2**). The

313 expression level of NGALU gradually decreased among IgAN 1-3 patients, and the expression

314 level of NGALU in IgAN-3 patients was significantly lower than that in IgAN-1 and MN patients

315 ($P < 0.05$). The ratio of NAGLU abundances among IgAN-1, IgAN-2, IgAN-3 and pMN in the

316 MS experiment was 1:0.52:0.48:0.82. This result was consistent with the MS results. GLA also

317 showed gradually decreased expression among IgAN 1-3 patients. This result was also consistent

318 with its decreasing levels in the MS experiment (IgAN-1: IgAN-2: IgAN-3: pMN,

319 1:0.70:0.52:0.81). GLA also showed different expression between IgAN-3 and pMN patients ($P <$

320 0.05).

321 **3.5 PRM validation of IgAN markers**

322   To validate the iTRAQ results, 64 urinary samples were collected, including 14 from IgAN-

323   1 (eGFR: > 90 ml/min/1.73 m^2), 29 from IgAN-2 (eGFR: 60-90 ml/min/1.73 m^2) and 21 from

324   IgAN-3 (eGFR: < 60 ml/min/1.73 m^2).

325   To evaluate LC–MS/MS system stability, a mixture of all urine samples was pooled as quality

326   control (QC) samples. The correlation map of QC samples showed that QC samples were highly

327   positively correlated, with an average Pearson correlation coefficient of 0.966 **(Fig. S3)**. The above

328   results showed the good repeatability and stability of the LC–MS/MS platform.

329   According to PRM analysis, 17 peptides that corresponded to 10 proteins were validated,

330   which showed the same trend as iTRAQ, including 2 upregulated proteins and 8 downregulated

331   proteins **(Figure 6 and Table 3)**. Complement Factor B (CFB) and complement component C8

332   alpha chain (C8A), as complements and related molecules, were verified to be upregulated. Among

333   the downregulated proteins, plasma serine protease inhibitor (SERPINA5), lymphocyte function-

334   associated antigen 3 (CD58) and mucosal addressin cell molecule 1 (MAdCAM1) presented a

335   gradually downward trend with the progression of IgAN, indicating a potential contribution to

336   monitoring the development of IgAN. DANSE2 and AXL were found to only significantly

337   decrease at IgAN-3, which may be associated with kidney injury at the end stage of IgAN.

338   The diagnostic values of 10 proteins were evaluated using ROC analysis. There were 7

339   proteins, and 9 showed an AUC > 0.75 compared with IgAN-2 and IgAN-3 with IgAN-1 **(Table**

340   **3)**. Meanwhile, the combination of CFB and MAdCAM1 showed an AUC of 0.963 (95% CI,

341   0.856-0.997)/0.915 (95% CI, 0.770-0.982) in distinguishing IgAN-2/3 from IgAN-1 **(Figure 7A**

342   **and 7B)**.

343   We further analysed whether these potential biomarkers correlated with the clinical test

344   results of IgAN. Spearman's correlation analysis showed that the urinary excretion of CFB and

345   C8A was negatively correlated with eGFR decline, while the other 8 proteins presented a positive

346   correlation with eGFR. The abundance of C8A, SERPINA5 and AXL also presented a stronger

347   correlation with 24-h urinary protein (24hUP) ($|r| > 0.3$). The 10 candidates, except LRG1, all

348   correlated with blood urea nitrogen (BUN) ($|r| > 0.2$), which indicated the occurrence of kidney

349   injury. Seven of 10 proteins, including CFB, C8A, DNASE2, SERPINA5, AXL, and EGF, were

350   also significantly associated with the evaluation of the MEST-C score ($|r| > 0.2$) and were most

351   significantly correlated with the T-score, which indicated interstitial fibrosis/tubular atrophy

352   **(Figure 7C)**.

353   **4. Discussion**

354   The aim of this study was to evaluate urine proteomics of patients with different stages of

355   IgAN, especially complements and complement-related proteins.

356   Activation of the complement pathway plays an important role in the pathogenesis of IgAN.

357   Alongside the development of targeted complement inhibitors in glomerular diseases [13], it is

358   necessary to better understand how the complement pathway is involved in IgAN progression. In

359   this study, we found that the urinary complements C3, MAC, and complement regulatory proteins

360   were increased with the progression of IgAN, indicating AP activation in the progression of IgAN.

361   In a previous urinary proteomic study of healthy individuals, Shao et al. [14] identified 1872

362   quantifiable proteins by 2D LC–MS/MS with the label-free quantitative method, including 26 of

363   27 complements reported in our study. In addition, Zhao et al. [15] identified all 27 complements

364   found in our study from pooled urinary samples of healthy individuals using the same proteomic-

365   based technology. In IgAN, IgA is mostly codeposited with C3 in the mesangium. MBL [16],

366   properdin and CFH deposition [17] were also found in the mesangium. A recent proteomic study

367   of microdissected glomeruli from progressive IgAN cases revealed significantly increased MAC

368 proteins, FHR5 and FHR2, compared with patients with stable clinical status [4]. In our study, 20

369 urinary complement proteins were found to be consistent with those previously found in the

370 microdissected glomeruli; notably, we found eight differentially expressed proteins of LP and

371 complement regulatory proteins that have not been identified in the microdissected glomeruli of

372 IgAN patients (Table S2).

373 Previous studies suggested that overactivation of AP-dependent complement amplification

374 could promote the formation of the MAC and lead to kidney injury in IgAN. According to the

375 iTRAQ results, CFH, CFHR2 and CFHR4 were found to have the highest expression in IgAN-3

376 (CFH: (IgAN1: IgAN2: IgAN3) = 1: 1.14: 2.41; CFHR2: (IgAN1: IgAN2: IgAN3) = 1: 1.25: 3.06,

377 CFHR4: (IgAN1: IgAN2: IgAN3) = 1: 1: 2.41). CFH is the major negative regulator of AP by

378 binding with C3b and inhibiting the formation of C3 convertase, which normally functions to avoid

379 excessive activation of the complement system. The CFHRs were sequentially similar to CFH and

380 could compete with CFH for binding with C3b. These proteins have been studied as potential risk

381 factors for IgAN [18]. Previous studies have reported that high levels of CFHR1, CFHR3 and

382 CFHR5 could increase C3b binding capacity and AP activation, resulting in complement-mediated

383 injury in IgAN [19,20]. Although there are fewer reports on urinary CFHR2 or CFHR4 in IgAN,

384 the functions of these two proteins also indicate the facilitation of complement system activation.

385 In vitro studies have demonstrated that CFHR4 initiates AP activation via the formation of active

386 C3 convertases on CFHR4-bound C3b [21]. Compared with other CFHRs, CFHR2 has a lower

387 affinity to compete with CFH in binding C3b or C3d but can form homologous dimers or

388 heterodimers with CFHR1 and CFHR5 [19]. Complexes of CFHR1, CFHR2 or CFHR5 have been

389 reported to increase the avidity for the ligands C3b, iC3b, and C3dg and enhance competition with

390 complement Factor H (CFH), eventually promoting AP activation on certain surfaces [22,23]. The

391   significant increase in CFH, CFHR2 and CFHR4 in IgAN-3 may reflect the potential function at

392   the end stage of IgAN.

393   There have been few studies on changes in serum or urinary LP proteins of the complement

394   cascade in IgAN patients. In this study, we identified four urinary LP proteins in IgAN patients.

395   Unlike MBL and MASP1, urinary MASP-2 and ficolin-2 gradually decreased with IgAN

396   progression. MASP-2 could directly cleave C3 while bypassing the usual sequence to activate C4

397   and/or C2, therefore playing an important role in the LP activation of the complement system [24].

398   A pilot study recently showed that nasoplimab, a MASP-2 inhibitor, could reduce proteinuria in

399   IgAN patients and maintain renal function, suggesting that MASP-2 activation may be involved

400   in the pathogenesis of IgAN [25]. The reasons for the downregulation of MASP-2 and ficolin-2 in

401   progressive IgAN patients are not fully understood. A British study compared levels of plasma LP

402   proteins between stable and progressive IgAN patients; specifically, M-ficolin, L-ficolin, MASP1

403   and MAp19 were increased, but MASP3 was decreased, in progressive IgAN patients, and there

404   was no difference in MASP-2 between IgAN and healthy controls [26]. These changes are thought

405   to be secondary to LP activation, with MASP2 consumption at sites of disease activity. Further

406   studies are required to assess the changes in urinary MASP2 and ficolin-2 in progressive IgAN

407   patients. In this study, the urinary complement profile of pMN patients with eGFR>90 ml/min/1.73

408   m^2 was analysed as a control. pMN is caused by autoantibodies that bind to antigens expressed by

409   podocytes. These autoantibodies, which are predominantly of the IgG4 subclass, mainly activate

410   the LP and AP [27]. Therefore, the abundance of urinary complements in pMN patients with

411   normal renal function was similar to that observed in IgAN-1 patients (Fig. 4). Meanwhile, 17

412   differential urinary proteins between pMN and IgAN were also identified in the discovery phase,

413   and their significance should be further investigated.

414   The proteins in Cluster 1 were increased with eGFR reduction, indicating that these proteins

415   were closely associated with disease severity in IgAN and could be used as noninvasive

416   biomarkers of disease progression. In Cluster 1, KEGG pathway analysis showed that the

417   complement and coagulation cascade pathways, immune disease pathway, and *Staphylococcus*

418   *aureus* infection were significantly enriched. A cohort study including 116 IgAN patients and 122

419   non-IgAN patients revealed that 68% of IgAN patients presented with *Staphylococcus aureus*

420   antigen, while non-IgAN patients had no *Staphylococcus aureus* antigen deposition [28]. Our

421   study revealed that the *Staphylococcus aureus* pathway was significantly activated with IgAN

422   progression and that *Staphylococcus aureus* interacted with MBL, C3, C4 and C5. Recently, a

423   study [29] reported that *Staphylococcus aureus* could activate LP by acting on MBL through the

424   glycol polymer wall containing teichoic acid on its surface.

425   Cluster 2 proteins were decreased with eGFR progression. Further pathway analysis revealed

426   that the first three enrichment pathways were cell adhesion molecules, focal adhesion and the

427   PI3K-Akt signalling pathway. Mesangial deposition of IgA and ECM expansion have been thought

428   to be the initiating event in IgAN pathogenesis. Our results showed that the PI3K-Akt signalling

429   pathway was significantly enriched at the early stage of IgAN. A gene array study [30] proposed

430   that differentially expressed genes between IgAN patients and healthy volunteers were mainly

431   involved in the PI3K-Akt signalling pathway, which is strongly related to cell proliferation.

432   As two glycosylation-related enzymes, NAGLU and GLA were also assessed by Western

433   blotting in IgAN 1-3 and MN patients, and the WB results were consistent with those of iTRAQ

434   quantitative proteomics. NAGLU is a type of glycosidase and is involved in the degradation of the

435   polysaccharide heparan sulfate (HS) by removing the terminal N-acetylglucosamine (GlcNac)

436   residue [31]. It has been reported that HS can promote fibrosis in the kidney [32]. The deficiency

437   of HS in mice was demonstrated to prevent profibrotic crosslinking of extracellular matrix and

438   recruitment of TGF-β1 [33,34], which was positively correlated with fibrotic area in renal tissue

439   of IgAN patients [35]. Therefore, the decline in NAGLU could result in the accumulation of

440   heparan sulfate (HS) [36] and may contribute to IgAN progression.

441   Alpha-galactosidase (GLA) is a lysosomal glycosidase and can catalyse the removal of α-

442   linked galactose from oligosaccharides, glycoproteins, and glycolipids during the salvage pathway

443   of galactose [37,38]. In humans, the deficiency of functional GLA could result in the accumulation

444   of galactosylated substrates (Gb3) in tissues, leading to Fabry disease, which is often accompanied

445   by a series of visceral diseases, including renal disease [39]. According to previous reports, IgAN

446   and Fabry disease may coexist [40-42]. However, the definite mechanism of GLA in IgAN is still

447   unknown. The WB results of NAGLU and GLA were consistent with their results based on iTRAQ

448   quantitative proteomics. This is the first study showing the changes in these two proteins in the

449   urine from IgAN patients, although their clinical significance remains to be further explored.

450   Among the DEPs validated in PRM, the increase in complement Factor B (CFB) and

451   complement component 8 a chain (C8A), consistent with iTRAQ, confirmed the activation of the

452   complement system in IgAN (**Figure 6**). CFB is an essential component of the alternative pathway,

453   providing an active subunit associated with C3b to form the C3 convertase [43]. Previous studies

454   have revealed increasing CFB or complement factor Bb (a fragment of CFB) in the circulation of

455   patients with IMN or IgAN [44]. In our study, CFB exhibited a negative correlation with eGFR

456   but a positive correlation with 24-h urine protein, which supports the association between urinary

457   CFB and AP activation in IgAN progression. C8A, as a component of the MAC, was significantly

458   increased in IgAN-2 and IgAN-3 compared with IgAN-1 in our study (**Figure 6**). The formation

459   of MAC or C5b-9 was reported to induce kidney cell injury, inflammation, and fibrosis [45].

460   Meanwhile, the efficiency of C5b-9 was also evaluated as a prognostic marker for IgAN. Several

461   studies on C5b-9 deposition demonstrated that almost all IgAN patients showed more intense and

462   diffuse C5b-9 deposition in the glomerulus and tubules than healthy controls [45-47]. Urine-based

463   proteomics studies have also suggested an increase in urinary C5b-9 levels in patients with IgAN.

464   Urinary C5b-9 levels were found to be associated with disease severity and inversely correlated

465   with eGFR [47-49]. The increase in CFB and C8A confirmed that the complement system,

466   including the AP and MAC pathways, could participate in biological processes during the

467   progression of IgAN at the urine level.

468   The combination of CFB and MAdCAM-1 was found to potentially distinguish IgAN patients

469   at different stages from weaker controls (IgAN-1). MAdCAM-1, as a transmembrane protein with

470   a complex structure, can combine three Ig domains and a mucin-like region between Ig domains

471   2 and 3. Moreover, there is also an IgA-like Ig domain in the MAdCAM-1 molecule, which could

472   be correlated with its expression in the area where most IgA antibodies are secreted [50].

473   MAdCAM-1 can regulate both the passage and retention of leukocytes and function in chronically

474   inflamed tissues [51]. Previous studies suggested that the tissue expression of adhesion molecules

475   in IgAN reflects continuous inflammatory renal activity, including vascular cell adhesion molecule

476   1 (VCAM-1) and intercellular adhesion molecule 1 (ICAM-1) [52,53]. However, few studies have

477   demonstrated the association between MAdCAM-1 and IgAN. A previous study detected soluble

478   MAdCAM-1 in the serum and urine of healthy donors, and the expression levels of MAdCAM-1

479   were similar to those of CAM, ICAM-1, and VCAM-1 [54]. The deficiency of MAdCAM-1 in

480   urine should be further studied for its potential diagnostic ability in the progression of IgAN.

481   After removing 14 highly abundant proteins in samples prior to quantitative proteomic

482   analysis, this study identified abundant complements and complement-related proteins in the urine

483   of IgAN patients with different CKD stages. To our knowledge, this is the first study to identify

484   an abundance of complements in the urine of IgAN patients. This is also the first study to

485   demonstrate alterations in urinary complements of AP and LP, and among the complements, the

486   major component involved in IgAN progression was MAC.

487   There are several limitations of this study. First, this study was a single-centre study with a

488   limited number of patients. Thus, a large-scale analysis, including healthy controls, IgAN patients

489   and patients with other related chronic kidney diseases, will be more comprehensive to confirm

490   the conclusions. Second, although CFB and C8A were validated by PRM, more related

491   complements, such as CFHR2 and CFHR4, should also be validated. IHC validations in IgAN

492   tissues were necessary to validate the conclusions. Third, a study on the function and mechanism

493   of the potential biomarkers for IgAN should be provided as well.

494   In conclusion, complement components were found in IgAN urine and increased with the

495   progression of IgAN. These findings indicated that the urine proteome may reflect the changes in

496   IgAN. In addition, a combination of CFB and MAdCAM-1 may be used as a potential urinary

497   biomarker for monitoring the development of IgAN. The findings of our study provide useful

498   information for future IgAN research and improve the understanding of the pathogenesis of IgAN.

499   ➢ **Acknowledgements**

500   We thank Ying Sun, Siqian Li, and Liling Lin for collecting specimens and Zhengguang Guo and

501   Wei Sun for their great help in analysing the experimental data.

502

503

504

505

506

507

508

509

510

511

512

513

References

515 [1] Floege J, Amann K. Primary glomerulonephritides. Lancet. 2016; 387:2036-48.

516 [2] Suzuki H, Kiryluk K, Novak J, Moldoveanu Z, Herr AB, Renfrow MB, Wyatt RJ, Scolari F,

517 Mestecky J, Gharavi AG, Julian BA. The pathophysiology of IgA nephropathy. J Am Soc Nephrol.

518 2011; 22:1795-803.

519 [3] Tortajada A, Gutierrez E, Pickering MC, Praga Terente M, Medjeral-Thomas N. The role of

520 complement in IgA nephropathy. Mol Immunol. 2019; 114:123-132.

521 [4] Paunas TIF, Finne K, Leh S, Marti HP, Mollnes TE, Berven F, Vikse BE. Glomerular

522 abundance of complement proteins characterized by proteomic analysis of laser-captured

523 microdissected glomeruli associates with progressive disease in IgA nephropathy. Clin

524 Proteomics. 2017;14; 14:30.

525 [5] Prikryl P, Vojtova L, Maixnerova D, Vokurka M, Neprasova M, Zima T, Tesar V. Proteomic

526 approach for identification of IgA nephropathy-related biomarkers in urine. Physiol Res. 2017;

527 66:621-632.

528 [6] Guo Z, Wang Z, Lu C, Yang S, Sun H, Reziw, Guo Y, Sun W, Yue H. Analysis of the

529 differential urinary protein profile in IgA nephropathy patients of Uygur ethnicity. BMC Nephrol.

530 2018; 19:358.

531 [7] J. Wu, W. Wang, Z. Chen, F. Xu, and Y. Zheng, "Proteomics applications in biomarker

532 discovery and pathogenesis for abdominal aortic aneurysm," (in eng), Expert Rev Proteomics, vol.

533 18, no. 4, pp. 305-314, Apr 2021, doi: 10.1080/14789450.2021.1916473.

534 [8] M. Wilhelm et al., "Mass-spectrometry-based draft of the human proteome," (in eng), Nature,

535 vol. 509, no. 7502, pp. 582-7, May 29 2014, doi: 10.1038/nature13319.

536 [9] Levey AS, Stevens LA, Schmid CH, Zhang YL, Castro AF 3rd, Feldman HI, Kusek JW, Eggers

537 P, Van Lente F, Greene T, Coresh J; CKD-EPI (Chronic Kidney Disease Epidemiology

538 Collaboration). A new equation to estimate glomerular filtration rate. Ann Intern Med. 2009;

539 150:604-12.

540 [10] Trimarchi H, Barratt J, Cattran DC, Cook HT, Coppo R, Haas M, Liu ZH, Roberts IS, Yuzawa

541 Y, Zhang H, Feehally J; IgAN Classification Working Group of the International IgA Nephropathy

542 Network and the Renal Pathology Society; Conference Participants. Oxford Classification of IgA

543 nephropathy 2016: an update from the IgA Nephropathy Classification Working Group. Kidney

544 Int. 2017; 91:1014-1021.

545 [11] Wiśniewski JR, Zougman A, Nagaraj N, Mann M. Universal sample preparation method for

546 proteome analysis. Nat Methods. 2009; 6:359-62.

547 [12] Guo Z, Liu X, Li M, Shao C, Tao J, Sun W, Li M. Differential urinary glycoproteome analysis

548 of type 2 diabetic nephropathy using 2D-LC-MS/MS and iTRAQ quantification. J Transl Med.

549 2015; 13:371.

550 [13] Andrighetto S, Leventhal J, Zaza G, Cravedi P. Complement and complement targeting

551 therapies in glomerular diseases. Int J Mol Sci. 2019; 20:6336.

552 [14] Shao C, Zhao M, Chen X, Sun H, Yang Y, Xiao X, Guo Z, Liu X, Lv Y, Chen X, Sun W, Wu

553 D, Gao Y. Comprehensive Analysis of Individual Variation in the Urinary Proteome Revealed

554 Significant Gender Differences. Mol Cell Proteomics. 2019; 18:1110-1122.

555 [15] Zhao M, Li M, Yang Y, Guo Z, Sun Y, Shao C, Li M, Sun W, Gao Y. A comprehensive

556 analysis and annotation of human normal urinary proteome. Sci Rep. 2017; 7:3024.

557 [16] Roos A, Rastaldi MP, Calvaresi N, Oortwijn BD, Schlagwein N, van Gijlswijk-Janssen DJ,

558 Stahl GL, Matsushita M, Fujita T, van Kooten C, Daha MR. Glomerular activation of the lectin

559 pathway of complement in IgA nephropathy is associated with more severe renal disease. J Am

560 Soc Nephrol. 2006; 17:1724-34.

561 [17] Miyazaki R, Kuroda M, Akiyama T, Otani I, Tofuku Y, Takeda R. Glomerular deposition and

562 serum levels of complement control proteins in patients with IgA nephropathy. Clin Nephrol.

563 1984; 21:335–40.

564 [18] Medjeral-Thomas NR, Lomax-Browne HJ, Pickering MC. Circulating complement factor H-

565 related protein 5 levels contribute to development and progression of IgA nephropathy. Kidney

566 Int. 2018; 94:150-158.

567 [19]E. Łukawska, M. Polcyn-Adamczak, and Z. I. Niemir, "The role of the alternative pathway of

568 complement activation in glomerular diseases," (in eng), Clin Exp Med, vol. 18, no. 3, pp. 297-

569 318, Aug 2018, doi: 10.1007/s10238-018-0491-8.

570 [20]M. Cserhalmi, A. Papp, B. Brandus, B. Uzonyi, and M. Józsi, "Regulation of regulators: Role

571 of the complement factor H-related proteins," (in eng), Semin Immunol, vol. 45, p. 101341, Oct

572 2019, doi: 10.1016/j.smim.2019.101341.

573   [21] M. Hebecker and M. Józsi, "Factor H-related protein 4 activates complement by serving as a

574   platform for the assembly of alternative pathway C3 convertase via its interaction with C3b

575   protein," (in eng), J Biol Chem, vol. 287, no. 23, pp. 19528-36, Jun 1 2012, doi:

576   10.1074/jbc.M112.364471.

577   [22] E. Goicoechea de Jorge et al., "Dimerization of complement factor H-related proteins

578   modulates complement activation in vivo," (in eng), Proc Natl Acad Sci U S A, vol. 110, no. 12,

579   pp. 4685-90, Mar 19 2013, doi: 10.1073/pnas.1219260110.

580   [23] A. Tortajada et al., "C3 glomerulopathy-associated CFHR1 mutation alters FHR

581   oligomerization and complement regulation," (in eng), J Clin Invest, vol. 123, no. 6, pp. 2434-46,

582   Jun 2013, doi: 10.1172/jci68280.

583   [24] Yaseen S, Demopulos G, Dudler T, Yabuki M, Wood CL, Cummings WJ, Tjoelker LW,

584   Fujita T, Sacks S, Garred P, Andrew P, Sim RB, Lachmann PJ, Wallis R, Lynch N, Schwaeble

585   WJ. Lectin pathway effector enzyme mannan-binding lectin-associated serine protease-2 can

586   activate native complement C3 in absence of C4 and/or C2. FASEB J. 2017; 31:2210-2219.

587   [25] Lafayette RA, Rovin BH, Reich HN, Tumlin JA, Floege J, Barratt J. Safety, Tolerability and

588   Efficacy of Narsoplimab, a Novel MASP-2 Inhibitor for the Treatment of IgA Nephropathy.

589   Kidney Int Rep. 2020; 5:2032-2041.

590   [26] Medjeral-Thomas NR, Troldborg A, Constantinou N, Lomax-Browne HJ, Hansen AG,

591   Willicombe M, et al. Progressive IgA nephropathy is associated with low circulating mannan-

592   binding lectin-associated serine protease-3 (MASP-3) and increased glomerular factor related

593   protein-5 (FHR5) deposition. Kidney Int Rep. 2018; 3:426–38.

594   [27] Ma H, Sandor DG, Beck LH Jr. The role of complement in membranous nephropathy. Semin

595   Nephrol. 2013; 33:531-42.

596 [28] Koyama A, Sharmin S, Sakurai H, Shimizu Y, Hirayama K, Usui J, Nagata M, Yoh K,

597 Yamagata K, Muro K, Kobayashi M, Ohtani K, Shimizu T, Shimizu T. Staphylococcus aureus cell

598 envelope antigen is a new candidate for the induction of IgA nephropathy. Kidney Int. 2004;

599 66:121-32.

600 [29] Kurokawa K, Takahashi K, Lee BL. The staphylococcal surface-glycopolymer wall teichoic

601 acid (WTA) is crucial for complement activation and immunological defense against

602 Staphylococcus aureus infection. Immunobiology. 2016;221: 1091-101.

603 [30] Cox SN, Sallustio F, Serino G, Pontrelli P, Verrienti R, Pesce F, Torres DD, Ancona N,

604 Stifanelli P, Zaza G, Schena FP. Altered modulation of WNT-beta-catenin and PI3K/Akt pathways

605 in IgA nephropathy. Kidney Int. 2010; 78:396-407.

606 [31]M. Uhlén et al., "Proteomics. Tissue-based map of the human proteome," (in eng), Science,

607 vol. 347, no. 6220, p. 1260419, Jan 23 2015, doi: 10.1126/science.1260419.

608 [32]G. Furini and E. A. M. Verderio, "Spotlight on the Transglutaminase 2-Heparan Sulfate

609 Interaction," (in eng), Med Sci (Basel), vol. 7, no. 1, Jan 4 2019, doi: 10.3390/medsci7010005.

610 [33]D. T. Talsma et al., "Endothelial heparan sulfate deficiency reduces inflammation and fibrosis

611 in murine diabetic nephropathy," (in eng), Lab Invest, vol. 98, no. 4, pp. 427-438, Apr 2018, doi:

612 10.1038/s41374-017-0015-2.

613 [34]A. Scarpellini et al., "Syndecan-4 knockout leads to reduced extracellular transglutaminase-2

614 and protects against tubulointerstitial fibrosis," (in eng), J Am Soc Nephrol, vol. 25, no. 5, pp.

615 1013-27, May 2014, doi: 10.1681/asn.2013050563.

616 [35]M. Yang, J. W. Liu, Y. T. Zhang, and G. Wu, "The Role of Renal Macrophage, AIM, and

617 TGF-β1 Expression in Renal Fibrosis Progression in IgAN Patients," (in eng), Front Immunol, vol.

618 12, p. 646650, 2021, doi: 10.3389/fimmu.2021.646650.

619   [36] E. E. A. Mohammed and E. M. Fateen, "Identification of Three Novel Homozygous NAGLU

620   Mutations in Egyptian Patients with Sanfilippo Syndrome B," Meta Gene, vol. 21, p. 100580,

621   2019/09/01/ 2019, doi: https://doi.org/10.1016/j.mgene.2019.100580.

622   [37] V. Lombard, H. Golaconda Ramulu, E. Drula, P. M. Coutinho, and B. Henrissat, "The

623   carbohydrate-active enzymes database (CAZy) in 2013," (in eng), Nucleic Acids Res, vol. 42, no.

624   Database issue, pp. D490-5, Jan 2014, doi: 10.1093/nar/gkt1178.

625   [38] A. I. Coelho, G. T. Berry, and M. E. Rubio-Gozalbo, "Galactose metabolism and health," (in

626   eng), Curr Opin Clin Nutr Metab Care, vol. 18, no. 4, pp. 422-7, Jul 2015, doi:

627   10.1097/mco.0000000000000189.

628   [39] K. Kok, K. C. Zwiers, R. G. Boot, H. S. Overkleeft, J. Aerts, and M. Artola, "Fabry Disease:

629   Molecular Basis, Pathophysiology, Diagnostics and Potential Therapeutic Directions," (in eng),

630   Biomolecules, vol. 11, no. 2, Feb 12 2021, doi: 10.3390/biom11020271.

631   [40] C. Whybra et al., "IgA nephropathy in two adolescent sisters heterozygous for Fabry disease,"

632   (in eng), Pediatr Nephrol, vol. 21, no. 9, pp. 1251-6, Sep 2006, doi: 10.1007/s00467-006-0176-5.

633   [41] L. Sun, X. Zi, Z. Wang, and X. Zhang, "IgA nephropathy with mimicking Fabry disease: A

634   case report and literature review," (in eng), Medicine (Baltimore), vol. 101, no. 42, p. e31060, Oct

635   21 2022, doi: 10.1097/md.0000000000031060.

636   [42] Y. V. Lerner, L. V. Tsoy, A. N. Grishina, and V. A. Varshavsky, "[Morphological

637   characteristics of renal changes in Fabry disease]," (in rus), Arkh Patol, vol. 84, no. 1, pp. 21-26,

638   2022, doi: 10.17116/patol20228401121. Morfologicheskaya kharakteristika izmenenii pochek pri

639   bolezni Fabri.

640   [43] K. Alfakeeh, M. Azar, M. Alfadhel, A. M. Abdullah, N. Aloudah, and K. O. Alsaad, "Rare

641   genetic variant in the CFB gene presenting as atypical hemolytic uremic syndrome and immune

642 complex diffuse membranoproliferative glomerulonephritis, with crescents, successfully treated
643 with eculizumab," (in eng), Pediatr Nephrol, vol. 32, no. 5, pp. 885-891, May 2017, doi:
644 10.1007/s00467-016-3577-0.

645 [44] M. F. Zhang et al., "Complement activation products in the circulation and urine of primary
646 membranous nephropathy," (in eng), BMC Nephrol, vol. 20, no. 1, p. 313, Aug 9 2019, doi:
647 10.1186/s12882-019-1509-5.

648 [45] J. J. E. Koopman, M. F. van Essen, H. G. Rennke, A. P. J. de Vries, and C. van Kooten,
649 "Deposition of the Membrane Attack Complex in Healthy and Diseased Human Kidneys," (in
650 eng), Front Immunol, vol. 11, p. 599974, 2020, doi: 10.3389/fimmu.2020.599974.

651 [46] D. Maixnerova, C. Reily, Q. Bian, M. Neprasova, J. Novak, and V. Tesar, "Markers for the
652 progression of IgA nephropathy," (in eng), J Nephrol, vol. 29, no. 4, pp. 535-41, Aug 2016, doi:
653 10.1007/s40620-016-0299-0.

654 [47] B. C. Yu et al., "Urinary C5b-9 as a Prognostic Marker in IgA Nephropathy," (in eng), J Clin
655 Med, vol. 11, no. 3, Feb 3 2022, doi: 10.3390/jcm11030820.

656 [48] K. Abe et al., "Intraglomerular synthesis of complement C3 and its activation products in IgA
657 nephropathy," (in eng), Nephron, vol. 87, no. 3, pp. 231-9, Mar 2001, doi: 10.1159/000045920.

658 [49] B. L. Neuen, M. Weldegiorgis, W. G. Herrington, T. Ohkuma, M. Smith, and M. Woodward,
659 "Changes in GFR and Albuminuria in Routine Clinical Practice and the Risk of Kidney Disease
660 Progression," (in eng), Am J Kidney Dis, vol. 78, no. 3, pp. 350-360.e1, Sep 2021, doi:
661 10.1053/j.ajkd.2021.02.335.

662 [50] A. M. Shyjan, M. Bertagnolli, C. J. Kenney, and M. J. Briskin, "Human mucosal addressin
663 cell adhesion molecule-1 (MAdCAM-1) demonstrates structural and functional similarities to the

664   alpha 4 beta 7-integrin binding domains of murine MAdCAM-1, but extreme divergence of mucin-

665   like sequences," (in eng), J Immunol, vol. 156, no. 8, pp. 2851-7, Apr 15 1996.

666   [51] J. Dando, K. W. Wilkinson, S. Ortlepp, D. J. King, and R. L. Brady, "A reassessment of the

667   MAdCAM-1 structure and its role in integrin recognition," (in eng), Acta Crystallogr D Biol

668   Crystallogr, vol. 58, no. Pt 2, pp. 233-41, Feb 2002, doi: 10.1107/s0907444901020522.

669   [52] C. Mrowka, B. Heintz, and H. G. Sieberth, "VCAM-1, ICAM-1, and E-selectin in IgA

670   nephropathy and Schönlein-Henoch syndrome: differences between tissue expression and serum

671   concentration," (in eng), Nephron, vol. 81, no. 3, pp. 256-63, 1999, doi: 10.1159/000045290.

672   [53] L. Wen, Z. Zhao, F. Li, F. Ji, and J. Wen, "ICAM-1 related long noncoding RNA is associated

673   with progression of IgA nephropathy and fibrotic changes in proximal tubular cells," (in eng), Sci

674   Rep, vol. 12, no. 1, p. 9645, Jun 10 2022, doi: 10.1038/s41598-022-13521-6.

675   [54] E. Leung et al., "Bioassay detects soluble MAdCAM-1 in body fluids," (in eng), Immunol

676   Cell Biol, vol. 82, no. 4, pp. 400-9, Aug 2004, doi: 10.1111/j.0818-9641.2004.01247.x.

677
678

679 **Declarations**

680 ➢ **Ethics approval and consent to participants**

681 The research was conducted ethically in accordance with the World Medical Association

682 Declaration of Helsinki. Patients have given their written informed consent. The study protocol

683 has been approved by the Ethics Committee of Peking Union Medical College Hospital (Ethics

684 approval number: JS-2573).

685 ➢ **Consent for publication**

686 Not applicable.

687 ➢ **Availability of data and materials**

688 All relevant data and its supplementary information files are included in the article. Besides, the

689 raw data for LC-MS/MS analysis can be download from Figshare online (details showed at the

690 supplemental files: 10.6084/m9.figshare.21685898, 21687299, 21688946, 21688979 and

691 21689000).

692 ➢ **Competing interests**

693 The authors have no conflicts of interest to declare.

694 ➢ **Funding**

695 This work was supported by the National Natural Science Foundation of China (No. 31200614),

696 the Beijing Municipal Science and Technology Project (D181100000118004), Youth Fund of

697 Peking Union Medical College Hospital (pumch201912152). The funders participated in the study

698 design, while had no role in data collection and analysis, decision to publish, or preparation of the

699 manuscript.

700 ➢ **Authors' contributions**

701 Xia Niu analyzed PRM analysis, and wrote the draft manuscript. Shuyu Zhang analyzed clinical

702 data, performed statistical analysis, and wrote the draft manuscript. Jianqiang Wu performed the

703 proteomic and western blot analysis. Jianling Tao participated in the study design and helped with

704 drafting of the manuscript. Wenling Ye reviewed the pathological diagnosis. Chen Shao directed

705 the study design. Guangyan Cai and Ke Zheng participated in the study design and coordination.

706 Mingxi Li conceived the study, participated in its design, and helped with drafting of the

707 manuscript. All authors read and approved the final manuscript.

708 **Appendix**

709 ➤ **Figure Legends**

710 Fig.1. The workflow of differential urinary proteome analysis and western blot validation.

711 Fig.2. Hierarchical clustering analysis of 747 urinary proteins from 4 pooled samples. A: Heatmap

712 of urinary proteins in IgAN subgroups and pMN group (two technical replicates). B: Mfuzz

713 analysis of urinary proteins among IgAN subgroups.

714 Fig.3. Functional analysis of urinary proteins in cluster 1 and cluster 2 of IgAN patients. (A) KEGG

715 pathway enrichment analysis of proteins in cluster 1. (B) Protein-protein interaction (PPI)

716 networks were created for cluster-1 proteins. (C) KEGG pathway enrichment analysis of

717 proteins in cluster 2. (D) PPI networks were created for cluster 2 proteins.

718 Fig.4. Comparison of urinary complements in IgAN 1-3 and pMN patients.

719 Fig.5. Western blotting validation of NAGLU and GLA in another patient cohort.

720 Fig.6. The PRM results of validated differential proteins.

721 Fig.7. The analysis of PRM results. (A) Receiver operating characteristic (ROC) analysis of IgAN-

722 2 and IgAN-1; (B) ROC curve analysis of IgAN-3 and IgAN-1. (C) Heatmap of correlations

723 between PRM results and clinical tests.

724 ➤ **Tables**

725 Table 1. Clinical and histopathological characteristics of patients enrolled in discovery and

726 validation phases.

727 Table 2. The relative abundance of all urinary complements in IgAN 1-3 and pMN patients.

728 Table 3. Validation proteins by parallel reaction monitoring.

729 ➢ **Supplementary Materials**

730 Supplemental Table 1. Identification and quantitation details of urinary proteins in IgAN and pMN

731 patients.

732 Supplemental Table 2. Differential complements between glomeruli and urine of IgAN patients.

733 Supplemental Figure 1. Functional analysis of urinary proteins upregulated in IgAN-1 patients

734 compared to pMN patients. (A)KEGG pathway enrichment analysis of 107 upregulated proteins

735 in IgAN-1 compared to pMN. (B)The PPI networks were created for 107 upregulated proteins in

736 IgAN-1 compared to pMN.

737 Supplemental Figure 2. The raw image of western blotting of NAGLU and GLA in another

738 patient cohort.

739 Supplemental Figure 3. Correlation of QC samples in PRM.

Figure 1

The workflow of differential urinary proteome analysis, western blotting and parallel reaction monitoring validation.
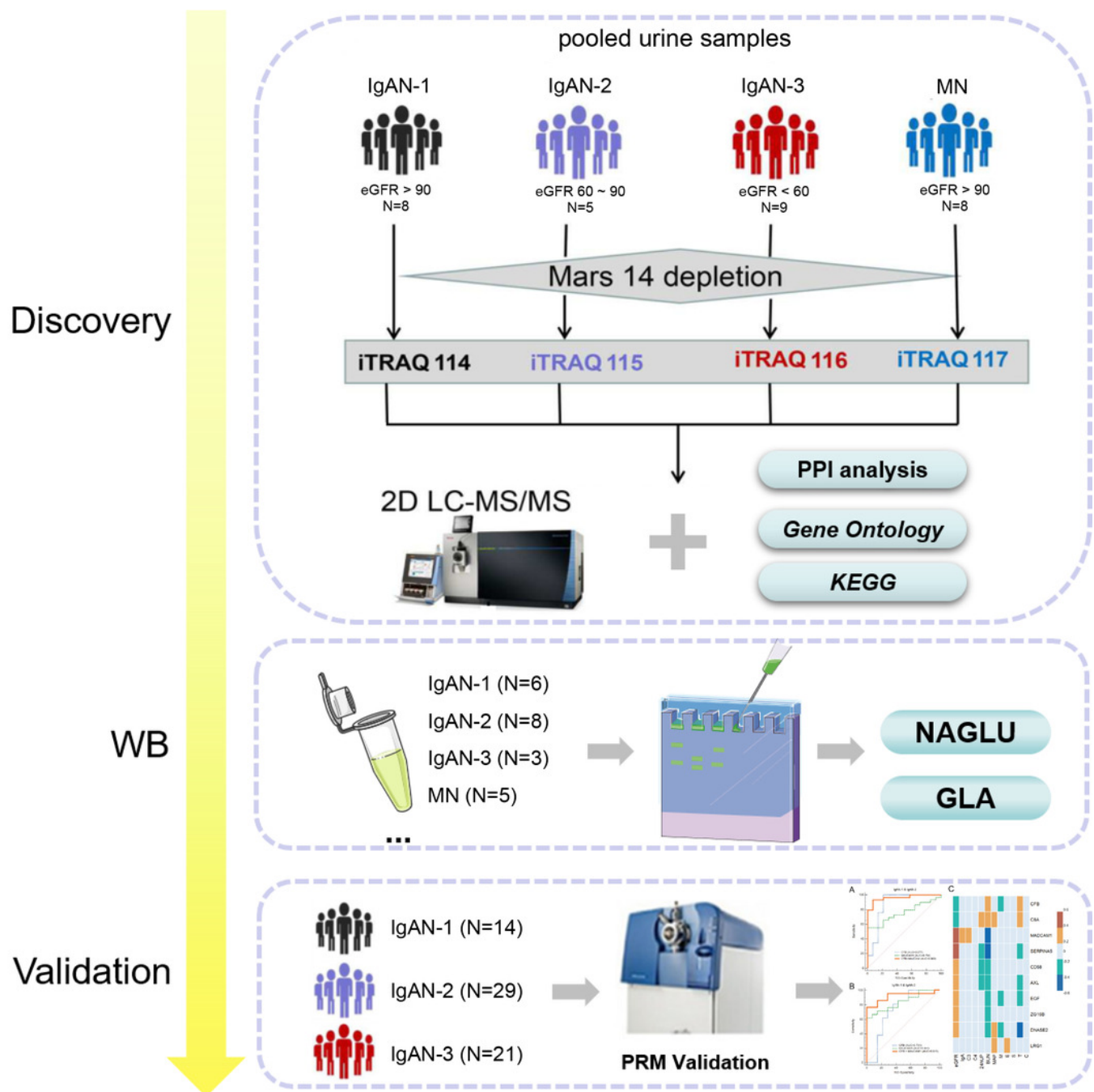
Figure 2

Hierarchical clustering analysis of 747 urinary proteins from 4 pooled samples.

(A) Heatmap of urinary proteins in IgAN subgroups and pMN group (two technical replicates). The color bar from orange to blue represented the fold change from increasing to decreasing of the proteins in four groups. **(B)** Mfuzz analysis of urinary proteins among IgAN subgroups. Proteins in cluster1 were increased with IgAN progression; Proteins in cluster2 were decreased with IgAN progression; Proteins cluster3(n=142) and Cluster4(n=291) showed no gradual changes with IgAN progression. Color bar represented Z-score change from -2 to 2.
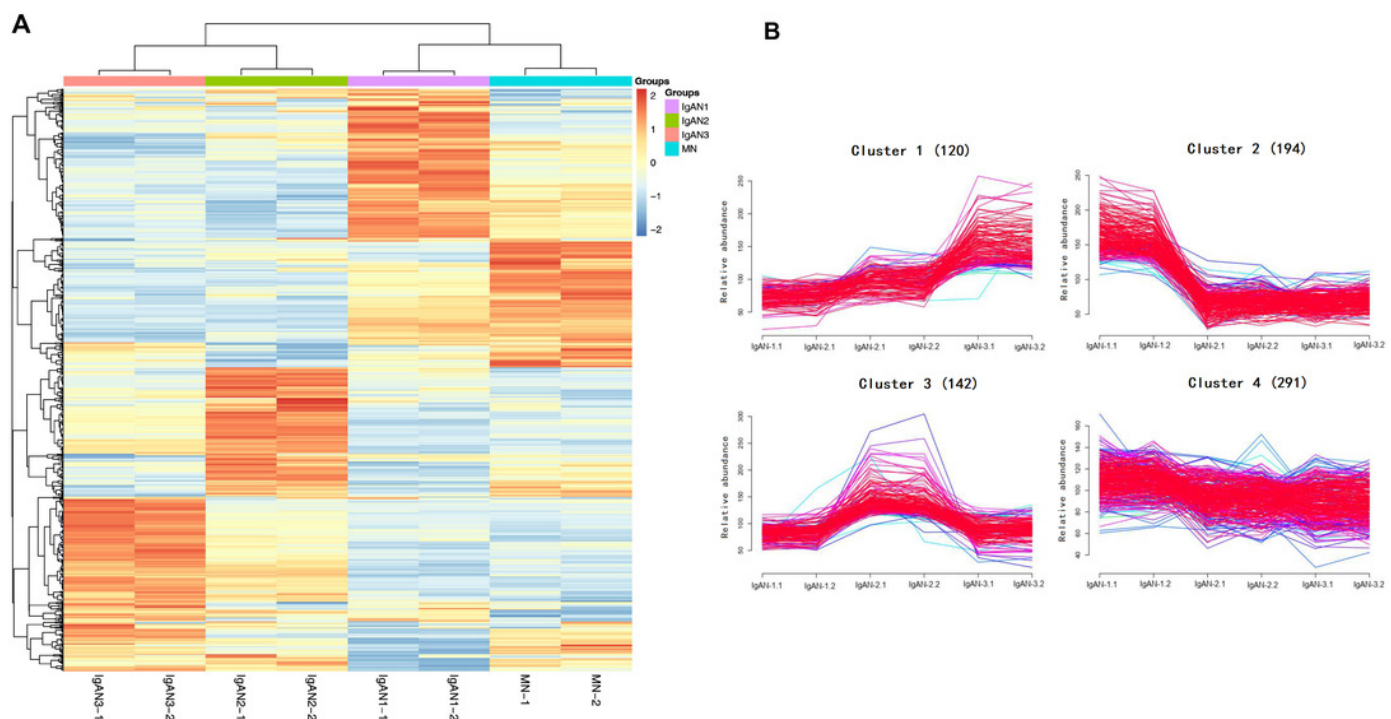
Figure 3

Functional analysis of urinary proteins in cluster 1 and cluster 2 of IgAN patients.

(A) KEGG pathway enrichment analysis of proteins in cluster 1. **(B)** Protein-protein interaction (PPI) networks were created for cluster 1 proteins. **(C)** KEGG pathway enrichment analysis of proteins in cluster 2. **(D)** PPI networks were created for cluster 2 proteins. In the KEGG enrichment analysis, the abscissa represented the percent of corresponding genes under each pathway classification (p value was noted in the bracket). The ordinate represented enrichment pathway. In the protein interaction networks, circle nodes represented for genes/proteins, rectangle for KEGG pathways. Green solid lines represented inhibition; red solid lines represented activation; blue dotted lines represented KEGG pathways. The significance of the pathways represented by -log (p value) was shown by color bar with dark blue as the most significant. The color of circle nodes from red to green represented the fold change from increasing to decreasing of the proteins.
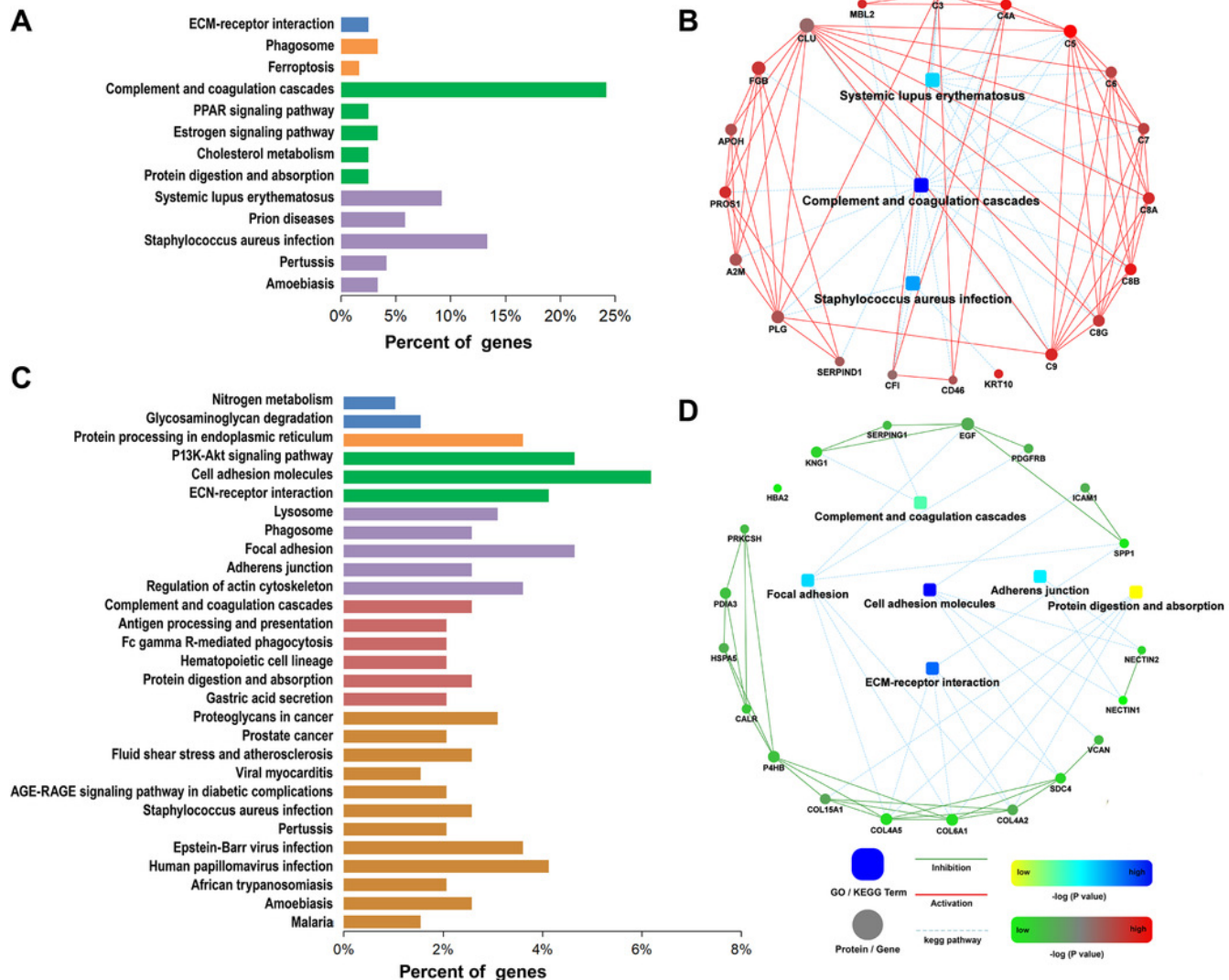
Figure 4

Comparison of urinary complements in IgAN 1-3 and pMN patients.

CP: Classical pathway; LP: Lectin pathway; AP: Alternative pathway; MAC: Membrane attack complex.
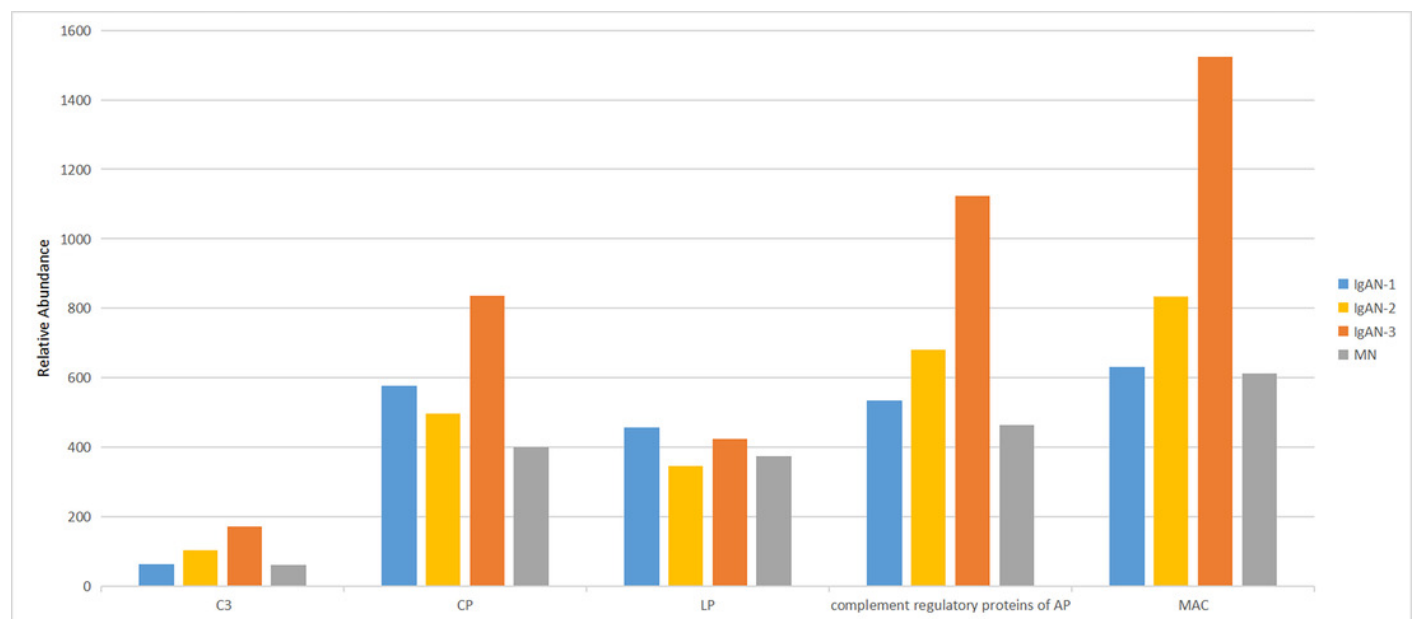
Figure 5

Western blotting validation of NAGLU and GLA in another patient cohort.

In the WB experiments, equal amount of urine protein from each individual sample was loaded. The validation set included IgAN-1 (n=6), IgAN-2 (n=8), IgAN-3 (n=3) and pMN (n=5) patients. Means and standard deviations were represented in the figure, and a nonparametric test were used to analysis the data. *Indicates a p value < 0.05.
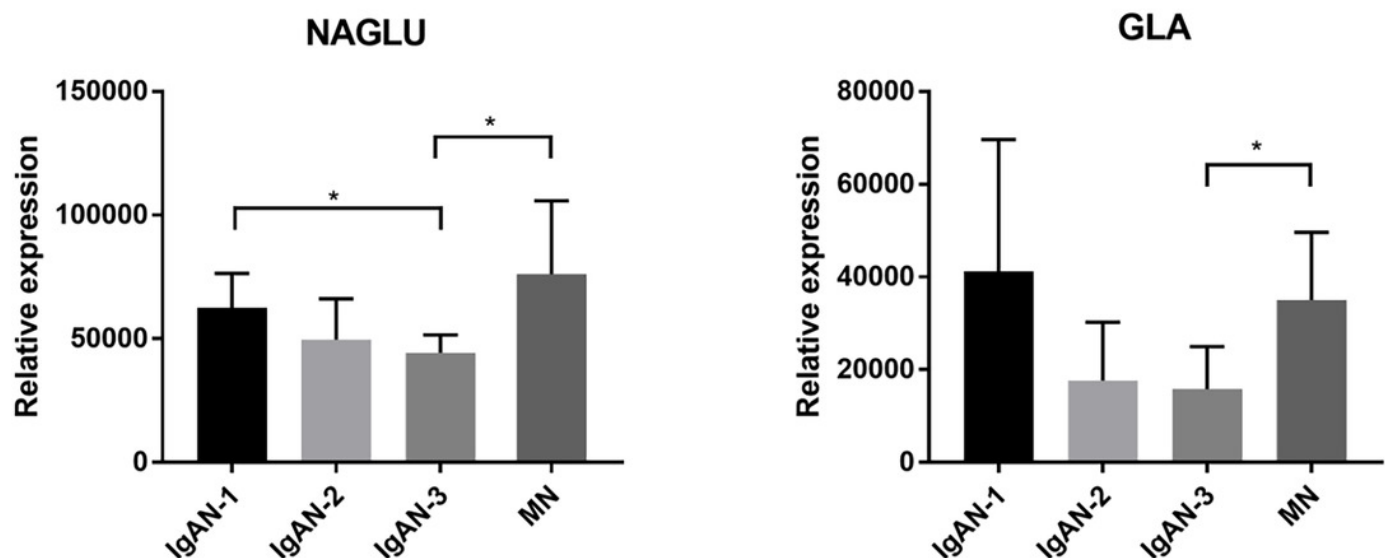
Figure 6

The PRM results of validated differential proteins.

IgAN-1: eGFR > 90 ml/min/1.73m^2, IgAN-2: eGFR: 60-90 ml/min/1.73m^2, IgAN-3: eGFR: 30-60 ml/min/1.73m^2. CFB, complement factor B; C8A, complement component C8 alpha chain; SERPINA5, plasma serine protease inhibitor; CD58, lymphocyte function-associated antigen 3; MADCAM1, mucosal addressin cell adhesion molecule 1; AXL, tyrosine-protein kinase receptor UFO; ZG16B, zymogen granule protein 16 homolog B; EGF, pro-epidermal growth factor; DNASE2, deoxyribonuclease-2-alpha; LRG1, leucine-rich alpha-2-glycoprotein.
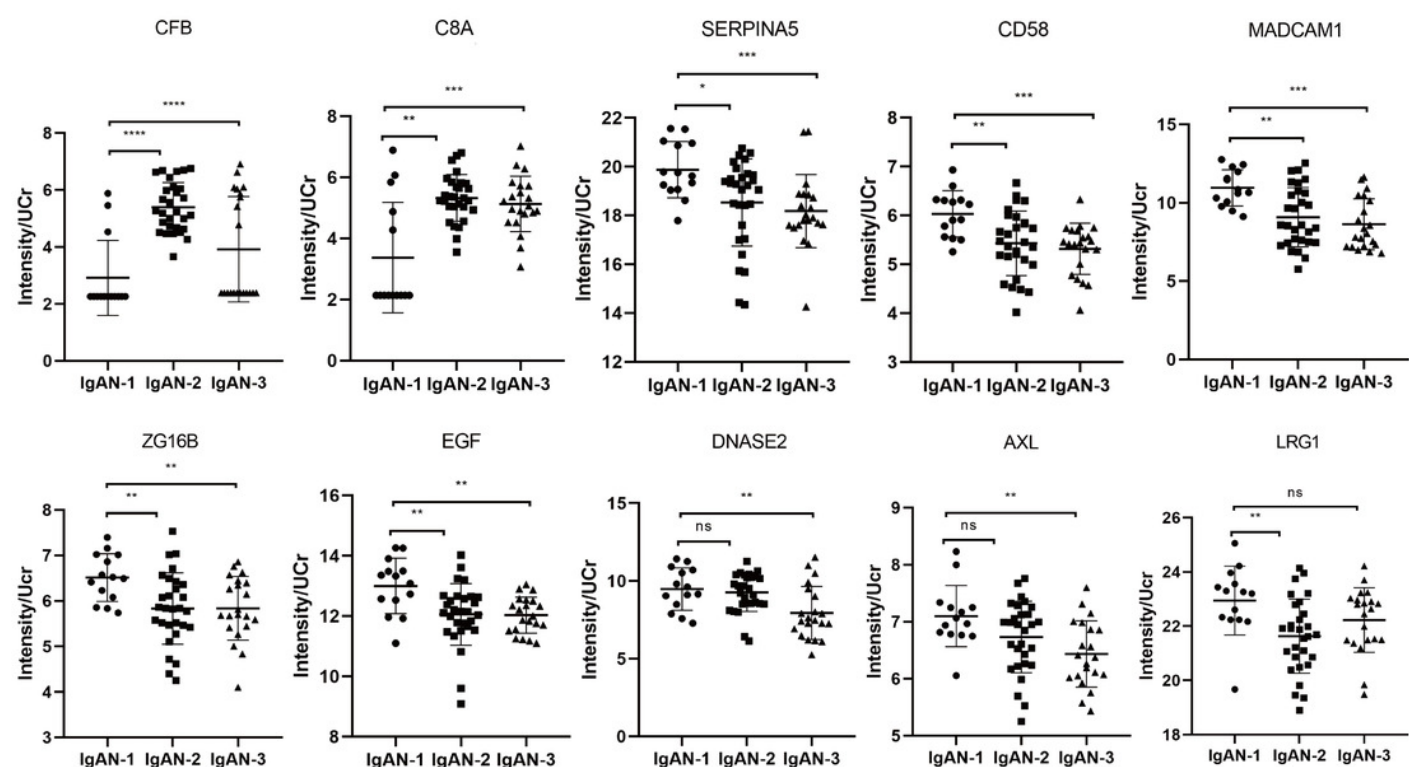
Figure 7

The analysis of PRM results.

(A) Receiver operating characteristic (ROC) analysis of IgAN-2 and IgAN-1; **(B)** ROC curve analysis of IgAN-3 and IgAN-1; **(C)** Heatmap of correlations between PRM results and clinical tests. eGFR, estimated glomerular filtration rate; C3: complement component 3; C4: complement component 4; 24hUP: 24-hours urinary protein; BUN, blood urine nitrogen; MAP, mean arterial pressure; M, mesangial hypercellularity; E, endocapillary cellularity; S, segmental sclerosis; T, interstitial fibrosis/tubular atrophy; C, crescents.
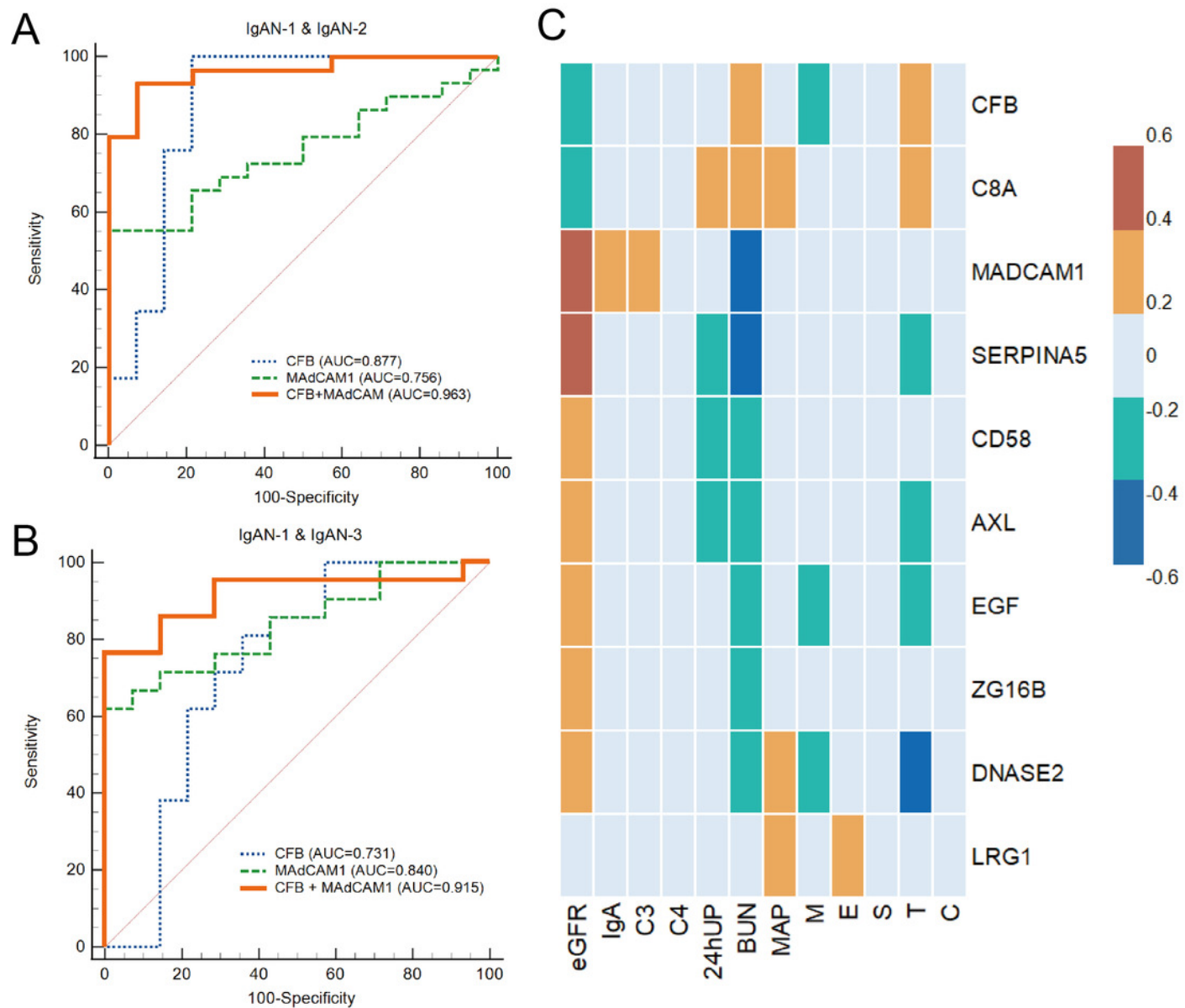
Clinical and histopathological characteristics of patients in discovery and validation phase.

N: number; 24 h UP: 24 hr urinary protein; SCr: serum creatinine; C3: complement 3; C4: complement 4.The five pathological variables in Oxford classification were scored as follow: mesangial score ≤ 0.5 (M0) or ⬜ 0.5 (M1), endocapillary hypercellularity absence (E0) or presence (E1), segmental glomerulosclerotic absence (S0) or presence (S1), tubular atrophy/interstitial fibrosis ≤ 25% (T0) or >25% (T1+T2), crescent absence (C0) or presence (C1+C2). Pa < 0.05 indicated comparison with IgAN-1; Pb< 0.05 indicated comparison with IgAN-2; Pc < 0.05 indicated comparison with IgAN-3.

Group	N	Gender (M/F)	Age (year)	24 h UP (g)	SCr (mmol/L)	eGFR (ml/min/1.73m^2)	C3 (g/L)	C4 (g/L)	Histopathological Characteristic
Discovery phase									
IgAN-1	8	5/3	33.25±6.86	1.36±0.84	74.10±13.62	112.20±11.55	1.05±0.16	0.21±0.04	$M_1E_{0-1}S_{0-1}T_0$-C_{0-1}
IgAN-2	5	4/1	39.20±12.66	2. 09±1.25	103.60±12.46a	74.78±11.32a	0.94±0.08	0.24±0.06	$M_1E_{0-1}S_1T_{0-2}$-C_1
IgAN-3	9	7/2	38.11±11.92	1.78±0.73	168.44±59.61a, b	45.37±11.76a, b	1.09±0.33	0.24±0.09	$M_1E_{0-1}S_1T_{0-2}$-C_{0-1}
MN	8	4/4	40.50±11.65	2.86±0.92a, c	68.63±17.28b, c	115.62±21.99b, c	1.18±0.21	0.26±0.09	MN I-II
WB validation									
IgAN-1	6	1/5	35.83±10.19	1.06±0.58	63.17±11.99	116.78±11.24	1.04±0.21	0.22±0.03	$M_1E_{0-1}S_{0-1}T_0$-C_{0-1}
IgAN-2	8	6/2	38.38±8.07	1.45±1.00	105.63±15.84a	72.47±7.86a	1.07±0.20	0.24±0.07	$M_1E_1S_1T_{0-2}$-C_1
IgAN-3	3	3/0	39.00±3.46	1.69±0.26	159.00±17.06a,b	47.01±7.22a, b	1.19±0.58	0.23±0.07	$M_1E_{0-1}S_1T_2$-C_1
MN	5	2/3	47.60±5.41	1.59±1.14	63.20±10.99b,c,d	115.5±19.44b,c,d	1.25±0.19	0.27±0.12	MN Ⅰ - Ⅱ
PRM Validation									
IgAN-1	14	8/6	35.57±12.8	1.48±0.69	73.14±10.42	110.73±22.67	1.12±0.18	0.21±0.09	$M_{0-1}E_{0-1}S_{0-1}T_{0-1}$-$C_{0-1}$
IgAN-2	29	17/12	39.24±11.63	1.86±1.11	102.72±18.67a	71.77±8.50a	1.13±0.16	0.23±0.06	$M_{0-1}E_{0-1}S_{0-1}T_{0-2}$-$C_{0-1}$
IgAN-3	21	12/9	45.14±13.35	2.13±1.15	128.29±16.60a	52.00±4.47a, b	1.12±0.14	0.24±0.06	$M_{0-1}E_{0-1}S_{0-1}T_{0-2}$-$C_{0-2}$

The relative abundance of all urinary complements in IgAN 1-3 and pMN patients

The complement proteins were divided into C3, CP (classical pathway), LP (lectin pathway), AP(alternative pathway) and MAC(membrane attack complex).

Complement	Uniprot	Description	IgAN-1	IgAN-2	IgAN-3	pMN	Molecular Weight(kDa)
C3	P01024	Complement 3	64	103	171	62	187.03
LP	P11226	Mannose binding protein	67	109	170	54	26.13
	Q15485	Ficolin-2	161	76	69	94	33.98
	P48740	Mannan-binding lectin serine protease 1	80	103	129	89	79.20
	O00187	Mannan-binding lectin serine protease 2	148	59	56	137	75.65
CP	P09871	Complement C1s	71	113	157	59	76.64
	Q9NZP8	Complement C1r	144	62	68	126	53.46
	Q9NPY3	Complement component C1q receptor	97	75	108	120	68.52
	P05155	Plasma protease C1 inhibitor	155	69	80	96	55.12
	P06681	Complement 2	52	103	202	44	83.21
	P0C0L4	Complement 4	59	76	221	44	192.65
Complement regulatory proteins of AP	P00751	Complement factor B	63	92	182	63	85.48
	P00746	Complement factor D	102	81	107	110	27.02
	P08603	Complement factor H	75	85	180	60	139.01
	P36980	Complement factor H-related protein 2	65	81	198	56	30.63
	Q92496	Complement factor H-related protein 4	76	76	183	66	37.27
	P05156	Complement factor I	98	89	148	65	65.71
	P27918	Properdin	57	176	123	45	51.24
	P08174	Complement decay-accelerating factor	85	103	112	100	41.37
MAC	P01031	Complement 5	54	76	229	42	188.19
	P13671	Complement 6	78	101	158	63	104.72
	P10643	Complement 7	73	114	130	83	93.46
	P07357	Complement component C8 alpha chain	68	92	189	51	65.12

P07358	Complement component C8 beta chain	59	85	198	59	67.00
P07360	Complement component C8 gamma chain	72	91	175	62	22.26
P02748	Complement 9	64	67	206	63	63.13
P15529	Membrane cofactor protein	79	105	127	89	43.72

Validated proteins by parallel reaction monitoring.

C8A, complement component C8 alpha chain; CFB, complement factor B; CD58, lymphocyte function-associated antigen 3; SERPINA5, plasma serine protease inhibitor; DNASE2, deoxyribonuclease-2-alpha; ZG16B, zymogen granule protein 16 homolog B; MADCAM1, mucosal addressin cell adhesion molecule 1; EGF, pro-epidermal growth factor; LRG1, leucine-rich alpha-2-glycoprotein; AXL, tyrosine-protein kinase receptor UFO.

Accession	Gene name	Peptides	iTRAQ Fold Change	PRM P value	PRM Fold change (IgAN-2/1)	AUC (IgAN-2/1)	PRM Fold change (IgAN-3/1)	AUC (IgAN-3/1)
P07357	C8A	YNPVVIDFEMQ PIHEVLR	2.344	0.004	1.579	0.788	1.523	0.776
P00751	CFB	LLQEGQALEYV CPSGFYPYPVQT R	2.181	0	1.851	0.899	1.345	0.857
P19256	CD58	VAELENSEFR	0.920	0.003	0.901	0.764	0.881	0.844
P05154	SERPI NA5	GFQQLLQELNQ PR EDQYHYLLDR	0.850	0.002	0.932	0.714	0.915	0.854
O00115	DNAS E2	AAAATGTIFTFR YLDESSGGWR	0.663	0.004	0.978	0.544	0.837	0.765
Q96DA0	ZG16B	ALINSPEGAVGR YFSTTEDYDHEI TGLR	0.645	0.01	0.895	0.764	0.896	0.793
Q13477	MADC AM1	GLDTSLGAVQS DTGR LPGLELSHR	0.631	0	0.829	0.783	0.788	0.857
P01133	EGF	IYFAHTALK LIEEGVDVPEGL AVDWIGR	0.660	0.003	0.927	0.761	0.926	0.816
P02750	LRG1	TLDLGENQLET LPPDLLR DGFDISGNPWIC DQNLSDLYR	0.496	0.009	0.943	0.791	0.969	0.684

		GQTLLAVAK						
P30530	AXL	TATITVLPQQPR	0.462	0.008	0.948	0.628	0.906	0.786